Arteriosclerosis, Thrombosis, and Vascular Biology

BASIC SCIENCES

Vascular Smooth Muscle Cell Subpopulations and Neointimal Formation in Mouse Models of Elastin Insufficiency

Chien-Jung Lin, Bridget M. Hunkins, Robyn A. Roth, Chieh-Yu Lin, Jessica E. Wagenseil, Robert P. Mecham

OBJECTIVE: Using a mouse model of Eln (elastin) insufficiency that spontaneously develops neointima in the ascending aorta, we sought to understand the origin and phenotypic heterogeneity of smooth muscle cells (SMCs) contributing to intimal hyperplasia. We were also interested in exploring how vascular cells adapt to the absence of Eln.

APPROACH AND RESULTS: We used single-cell sequencing together with lineage-specific cell labeling to identify neointimal cell populations in a noninjury, genetic model of neointimal formation. Inactivating Eln production in vascular SMCs results in rapid intimal hyperplasia around breaks in the ascending aorta's internal elastic lamina. Using lineage-specific *Cre* drivers to both lineage mark and inactivate Eln expression in the secondary heart field and neural crest aortic SMCs, we found that cells with a secondary heart field lineage are significant contributors to neointima formation. We also identified a small population of secondary heart field-derived SMCs underneath and adjacent to the internal elastic lamina. Within the neointima of SMC-Eln knockout mice, 2 unique SMC populations were identified that are transcriptionally different from other SMCs. While these cells had a distinct gene signature, they expressed several genes identified in other studies of neointimal lesions, suggesting that some mechanisms underlying neointima formation in Eln insufficiency are shared with adult vessel injury models.

CONCLUSIONS: These results highlight the unique developmental origin and transcriptional signature of cells contributing to neointima in the ascending aorta. Our findings also show that the absence of Eln, or changes in elastic fiber integrity, influences the SMC biological niche in ways that lead to altered cell phenotypes.

GRAPHIC ABSTRACT: A graphic abstract is available for this article.

Key Words: cell differentiation ■ elastin ■ extracellular matrix ■ myocytes ■ neointima ■ smooth muscle

Neointima, the accumulation of fibromuscular tissue luminal to the internal elastic lamina (IEL), occurs in multiple forms of obstructive cardiovascular diseases, including coronary artery restenosis after percutaneous interventions, coronary artery bypass graft occlusion (especially vein grafts),[1,2] arteriovenous fistula occlusion,[3] and supravalvular aortic stenosis in Williams-Beuren syndrome patients.[4] These diverse forms of neointimal formation share a common attribute: a compromised IEL in a vessel exposed to arterial pressure. In percutaneous interventions, the disruption of the IEL occurs in the coronary artery. In coronary artery bypass or arteriovenous fistula surgery, veins (which intrinsically have a discontinuous IEL) are exposed to an arterial environment. In supravalvular aortic stenosis, patients with mutations in the Eln (elastin) gene exhibit IEL disruption in the ascending aorta, where extensive neointima formation occurs.[4]

See accompanying editorial on page 2906
See cover image

Animal models of neointimal hyperplasia typically involve induced injuries, such as endothelial cell (EC) denudation or arterial ligation. We recently developed a novel mouse genetic model for neointimal formation that does not include vascular injury. Mice with smooth muscle cell (SMC)-specific Eln deletion develop a fragmented IEL in the

Correspondence to: Robert P. Mecham, PhD, Department of Cell Biology and Physiology, Washington University School of Medicine, 660 S Euclid Ave, CB 8228, St Louis, MO 63110. Email bmecham@wustl.edu
The Data Supplement is available with this article at https://www.ahajournals.org/doi/suppl/10.1161/ATVBAHA.120.315681.
For Sources of Funding and Disclosures, see page 2903.

Arterioscler Thromb Vasc Biol is available at www.ahajournals.org/journal/atvb

Nonstandard Abbreviations and Acronyms

Acta2	smooth muscle actin
Cnn1	calponin
EC	endothelial cell
Eln	elastin
FACS	fluorescence-activated cell sorter
IEL	internal elastic lamina
Myh11	myosin heavy chain 11
NC	neural crest
scRNA-seq	single-cell RNA sequencing
SHF	secondary heart field
SMC	smooth muscle cell

Highlights

- The absence of elastin in the aortic media leads to neointima formation.
- Secondary heart field-derived cells contribute disproportionately to aortic neointima formation compared with neural crest-derived smooth muscle cells.
- A new secondary heart field-derived smooth muscle cell population was identified underneath and directly adjacent to the internal elastic lamina.
- Single-cell sequencing identified 3 unique smooth muscle cell populations in the aortic wall, 2 of which specifically localize to the neointima in a genetic disease model.
- The absence of elastin alters the transcriptional phenotype of the major smooth muscle cell populations in the aortic wall.

ascending aorta with associated neointima.[5] As IEL disruption is an underlying component in neointima pathogenesis, the mechanistic insights gained from this genetic model are likely to apply to other forms of intimal lesion formation. This study uses lineage-specific *Cre* drivers to examine how Eln deletion in SMCs of different embryonic origins contributes to IEL formation, vessel integrity, and neointimal formation. We also use single-cell RNA sequencing (scRNA-seq) to define the cellular and transcriptomic landscape of vascular cells in response to Eln deletion. Our results show a complex SMC response that suggests phenotypic changes associated with cells that leave the medial layer and populate the neointima. We postulate that the presence or absence of Eln, or changes in elastic fiber integrity, influences the SMC biological niche in ways that lead to altered cell phenotypes and enhanced disease outcomes.

MATERIALS AND METHODS

The single-cell sequencing data sets will be made publicly available at the Gene Expression Omnibus website. The authors declare that all other supporting data are available within the article and its Data Supplement.

Mice, Genotyping, and Survival Analysis

Eln^{f} mice reported previously[5] were bred to various *Cre* lines and maintained in mixed backgrounds. *Tagln*C*re* (The Jackson Laboratory no. 004746),[6,7] *Isl1Cre* (The Jackson Laboratory no. 024242),[8] *Wnt1Cre* (*Wnt1Cre2*, The Jackson Laboratory no. 022137),[9] and *ROSA26*$^{mT/mG}$ mice (The Jackson Laboratory no. 007576)[10] were described previously. Experimental mice were compared with littermate controls. *Eln*$^{f/f}$ and *Eln*$^{f/+}$ mice were combined as controls in most instances. Both sexes were used for all studies. All animal studies were approved by the Institutional Animal Care and Use Committee at Washington University. TransnetYX, Inc performed genotyping. The *Eln* alleles were amplified with the following primers: ElnF: CCATGTGGGTGCTGTAAGCT, ElnR: GCAGTGCTGGCTCCCA, Probe 1, wild type: CCTGCCTGAGTTCTCA, Probe 2, LoxP floxed: AGGTCGACATAACTTCG. Genotyping for *Cre*, *TagInCre*, *Wnt1Cre*, and *ROSA26*$^{mT/mG}$ alleles was performed with TransnetYX's proprietary primers. Tissue sampling for genotyping was generally performed between 5 and 14 days after birth or at the time of euthanize, whichever was earlier. For the survival analysis, the day of death was defined as the day the animal was found dead, or the midpoint between the days the animal was last observed and the day found missing. The survival data were analyzed using the Log-rank test with Prism 8 software (Graphpad Software, San Diego, CA). For analysis of Mendelian ratios, the expected number of recovered mutants (*Isl1Cre;Eln*$^{f/f}$ or *Wnt1Cre;Eln*$^{f/f}$) and respective nonmutants (*Eln*$^{f/+}$, *Eln*$^{f/f}$, *Isl1Cre;Eln*$^{f/+}$ or *Wnt1Cre;Eln*$^{f/+}$) were analyzed using the χ^2 test. The *Isl1Cre;Eln*$^{f/+}$ and *Wnt1Cre;Eln*$^{f/+}$ animals were pooled with *Eln*$^{f/+}$ and *Eln*$^{f/f}$ animals because there was no difference in survival. A P value of <0.05 was considered significant.

Human Pathological Samples

Deidentified archival pathological specimens were retrieved, and the slides were reviewed by a cardiovascular pathologist (C.-Y. Lin) to confirm the diagnosis and histology. H&E and Verhoeff-van Gieson staining were performed by the Washington University Anatomic and Molecular Pathology core labs. Unstained sections were cut from the archival formalin-fixed, paraffin-embedded tissue in 5 µm thickness on positively charged slides. Immunostaining was performed according to the methods below. The coronary artery neointimal tissue was obtained from the explanted heart during a repeat orthotopic heart transplant for a 16-year-old female patient who underwent the first transplant 4 years prior. The control coronary artery was obtained from the autopsy of a 67-year-old male patient with coronary artery disease and ischemic cardiomyopathy. As determined by H&E staining of adjacent slides, a morphologically normal segment was chosen for IGFBP2 (insulin-like growth factor-binding protein-2) staining. The Washington University Institutional Review Board approved the study.

Histology and Immunostaining

Harvested tissues were fixed overnight at 4 °C in 4% paraformaldehyde in PBS solution or 10% neutral buffered formalin (Thermo Fisher Scientific, Waltham, MA). For frozen sections, fixed samples were embedded in Optimum Cutting Temperature Compound (Sakura Finetek), flash-frozen, and sectioned at 5 µm thickness with a cryostat. For paraffin sections, fixed tissue

was dehydrated, paraffinized with a tissue processor, embedded, and sectioned at 5 µm thickness using a microtome.

For immunohistochemistry, paraffin tissue sections were rehydrated, immersed in antigen retrieval solution (10 mmol/L Tris, 1 mmol/L EDTA, pH 9), and then heated for 10 minutes in a pressure cooker. After cooling down to room temperature, the slides were blocked with 0.3% hydrogen peroxide and the Mouse on Mouse blocking reagent (Vector Labs), followed by incubation with the primary antibody for 1 hour at room temperature in the Mouse on Mouse diluent. Following the manufacturer's instructions, visualization was accomplished using biotin-conjugated secondary antibodies using the Mouse on Mouse and the streptavidin-based ABC Kits (Vector Labs). Nuclei were counterstained with hematoxylin. Stained slides were dehydrated, cleared, and mounted with Cytoseal 60 (Thermo Fisher), Permount solution (Thermo Fisher), or VectaMount Permanent (Vector Labs). For immunofluorescence, following antigen retrieval, slides were quenched with 0.3 mol/L glycine. They were blocked with Mouse on Mouse blocking reagent or 2% normal donkey serum (Sigma), incubated with the primary antibody for 1 hour at room temperature, then incubated with Alexa 488- or Alexa 594-conjugated secondary antibodies (Life Technologies) for 1 hour at room temperature in the dark. Nuclei were counterstained with Hoechst 34580 (5 µmol/L, Life Technologies) or DAPI (Sigma). Elastic fibers were visualized with Alexa Fluor 633 hydrazide (Thermo Fisher). Primary antibodies used include mouse anti-smooth muscle α-actin (1:200, 1A4, Sigma-Aldrich), rabbit anti-Myh11 (myosin heavy chain; 5 µg/mL, JA03-35, Novus Biologicals), rabbit anti-Cnn1 (calponin; 5 µg/mL, SI67-01, Novus Biologicals), rabbit anti-Ptch1 (6 µg/mL, NB1-71662, Novus Biologicals), rabbit anti-Birc5 (3 µg/mL, 71G4B7, no. 2808, Cell Signaling), and rabbit anti-Igfbp2 (3 µg/mL, EPR18012-257, Abcam). The Verhoeff-van Gieson staining was performed by first overstaining sections with alcoholic hematoxylin-ferric chloride-iodine, followed by differentiation with ferric chloride and then sodium thiosulfate. Before dehydration, the slides were counterstained with van Gieson solution and mounted with Permount solution (Thermo Fisher).

Transmission Electron Microscopy

Arteries used for transmission electron microscopy were fixed in 2.5% glutaraldehyde and 0.1 mol/L sodium cacodylate at 4 °C overnight. They were sent to Washington University's Center for Cellular Imaging for processing and thin sectioning following standard protocols. Images were taken using a JEOL JEM-1400Plus transmission electron microscope with Advanced Microscopy Techniques XR111 high-speed, 4000×2000 pixel, phosphor-scintillated, 12-bit charge-coupled device camera. IEL thickness was measured at 7 locations of high Eln density in 2 ascending aorta of each group and averaged. IEL density was measured by manually outlining the outer edges of the IEL in the image, thresholding the image, and then determining the percentage of thresholded pixels in the IEL area for 2 ascending aorta in each group. Images at ×800 to ×3000 magnification were analyzed using Image J software (National Institutes of Health). Significant differences were not determined due to the low N.

Vascular Casting

Mice were euthanized by CO_2, and their chest wall was excised. Blood was drained from the vasculature by injecting PBS through the left ventricular apex after transecting the left common iliac artery. Yellow latex (Ward's Science) was then injected through the left ventricle.[11] Mice were fixed in 10% neutral buffered formalin at 4 °C overnight, followed by fine dissection to reveal the aorta and aortic arch arteries.

Single-Cell Suspension Preparation

Live single-cell preparation was performed following previously described methods[12] with minor modifications. Briefly, postnatal day (P) 8 mice were euthanized and perfused with cold PBS via cardiac ventricular puncture. The aorta was dissected out on ice-cold PBS with the perivascular fat and cardiac muscle removed. The ascending aorta was isolated proximal to the innominate artery. Ascending aorta from 4 *TagInCre;Eln*$^{f/f}$ pups were pooled. For the control group, 3 aorta were used (2 *Eln*$^{f/+}$, 1 *Eln*$^{f/f}$). The tissue was minced into small pieces and incubated at 37 °C for ≈20 minutes with gentle shaking in Hank's balanced salt solution with calcium and magnesium (Life Technologies) containing DNase I (90 U/mL), collagenase I (675 U/mL), collagenase XI (187.5 U/mL), and hyaluronidase (90 U/mL; all from Sigma). Enzymatic digestion was stopped by the addition of 2 mmol/L EDTA. The suspension was passed through a 70 µm strainer and washed 5 times with RPMI 1640 medium with 5% fetal bovine serum (Life Technologies). The cells were spun down at 800×g at 4 °C and resuspended in the RPMI 1640 buffer. For discriminating dead cells, the cells were prestained with DAPI just before flow cytometry. Flow cytometric analysis and sorting were performed using a BD FACSAria III sorter. The sorted cells (106 177 events for the *TagInCre;Eln*$^{f/f}$ group and 51 050 events for the control group) were resuspended in fluorescence-activated cell sorter (FACS) buffer containing 0.04% BSA in PBS at 1000 cells/µL and submitted to the McDonnell Genome Institute for library preparation and sequencing.

Library Preparation and scRNA-Seq

Library preparation using the 10X Chromium 3' V3 kit, sequencing using an Illumina NovaSeq sequencer, and demultiplex using the CellRanger pipeline were performed by the McDonnell Genome Institute at Washington University in St Louis.

scRNA-Seq Data Analysis

The demultiplexed data set underwent preprocessing, dimensional reduction, clustering, and analysis using the R package Seurat v4.0.0.[13] Cells with the expression of <500 genes or those with >25% expression of mitochondrial genes were removed from the analysis.

The data for *TagInCre;Eln*$^{f/f}$ and Ctrl were integrated using reciprocal principal component analysis (PCA). Individual data sets were normalized (NormalizeData), and variable features were identified (FindVariableFeatures, vst selection method). Features were selected that are repeatedly variable across data sets (SelectIntegrationFeatures), then each data set was scaled (ScaleData), and PCA was run (RunPCA) based on these features. Anchors were identified (FindIntegrationAnchors, reciprocal PCA reduction method), and the data sets were integrated based on these anchors. The standard Seurat workflow was then run for visualization and clustering of the integrated data set using ScaleData, RunPCA, RunUMap (PCA reduction method, based on PCs 1–10), FindNeighbors (PCA reduction method, dimension =10), and FindClusters (resolution =0.5).

Hierarchical clustering analysis of the integrated clusters was performed with the BuildClusterTree function. Marker genes for each integrated cluster compared with all other clusters were determined with FindAllMarkers using a Wilcoxon rank-sum test on the RNA assay. Differential gene expression between genotypes for each cluster was determined using FindMarkers. Genes expressed in a minimum of 25% of cells in a group and a log-fold change threshold of 0.25 were selected. Volcano, dot, and violin plots of the log normalized data from the RNA assay were generated using EnhancedVolcano,[14] DotPlot, and VlnPlot.

Differential proportion analysis for the integrated cell clusters was performed according to Farbehi et al[15] with w=0.1, t=100 000. Reactome gene set analysis was performed according to Griss et al.[16] Reactome pathway analysis was performed with clusterProfiler and ReactomePA packages.[17]

Statistical Analysis

Marker genes for clusters were identified with the Seurat FindAllMarkers method with a minimum log-fold change threshold of 0.25 and a minimum percentage of expressing cells of 0.25; *P* values were computed using a Wilcoxon rank-sum test. Pathway enrichment analysis was performed with the ReactomePA enrichPathway method; *P* values were derived from a hypergeometric test and adjusted using a Benjamini-Hochberg procedure. An adjusted *P* value of <0.05 was considered significant.

RESULTS

Neointima in *TagInCre;Eln$^{f/f}$* Ascending Aorta Arises Shortly After Birth From Vascular Cells That Express SMC Markers

Previous studies showed that mice with an Eln null allele in vascular SMCs (*TagInCre;Eln$^{f/f}$*) develop substantial neointima in the ascending aorta and die between P9 to P18 from cardiac problems secondary to a severe aortic arch coarctation.[5] These animals lack circumferential elastic lamina in the medial layer but have a noticeable, fragmented IEL, with neointimal formation occurring at areas where the IEL is absent or disrupted.[5] Using the *ROSA26$^{mT/mG}$* reporter, we demonstrated that the neointimal cells or their progenitors expressed *TagInCre* (Figure 1A), consistent with a smooth muscle lineage. Immunostaining for smooth muscle-associated protein, including Acta2 (smooth muscle actin [SMA]), Cnn1, and smooth muscle Myh11, confirmed that neointimal cells expressed these mature SMC markers (Figure 1B).

To learn whether neointima is present at birth, we compared the aortic wall structure of control and *TagInCre;Eln$^{f/f}$* animals at P2. At this developmental age, the ascending aorta from both genotypes had patchy, disrupted elastic layers in the tunica media with no neointima (Figure 2A). With postnatal development, the IEL increased in thickness and density in both groups (Table I in the Data Supplement) but remained thin and disrupted in the *TagInCre;Eln$^{f/f}$* aorta compared with control (Figure 2B). By P8, *TagInCre;Eln$^{f/f}$* animals, but not controls

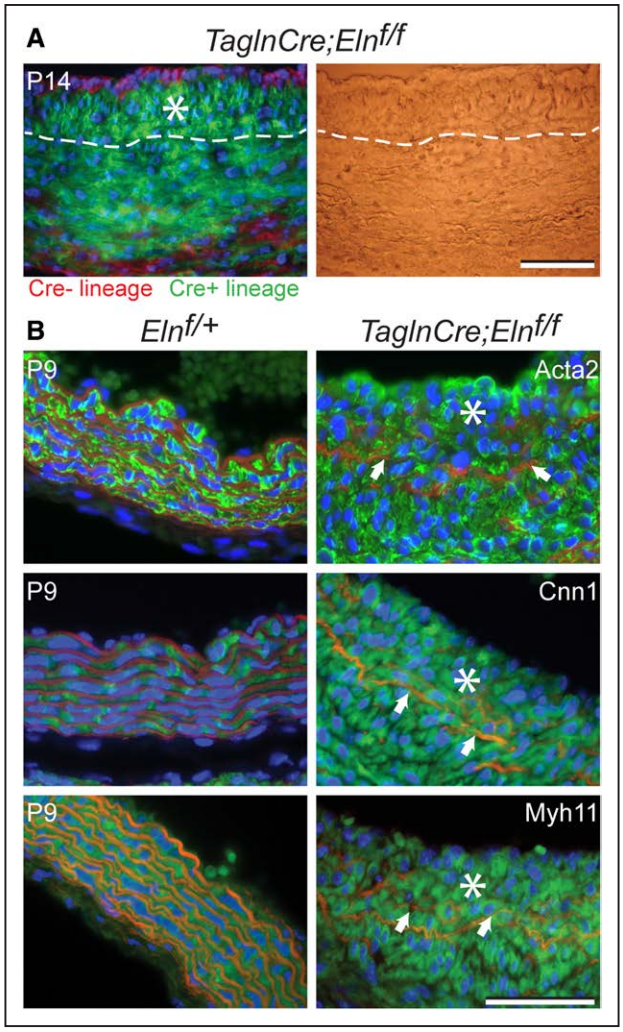

Figure 1. Smooth muscle cells (SMCs) populate the neointima in *TagInCre;Eln$^{f/f}$* ascending aorta.
A, Aortas from 14-d (P14) *TagInCre;Eln$^{f/f}$;ROSA26$^{mT/mG}$* mice showing that cells populating the neointima (*) are from the SMC lineage (green). The internal elastic lamina (IEL) is indicated by a dashed line based on the brightfield image (**right**) from the same section. Scale bar=50 µm. **B**, Representative immunofluorescent images of P9 *TagInCre;Eln$^{f/f}$* aortic sections (lacking the *ROSA26$^{mT/mG}$* allele) stained with antibodies to the SMC markers Acta2 (smooth muscle actin), Cnn1 (calponin), and Myh11 (myosin heavy chain 11), confirming the SMC lineage of neointimal cells. Green color indicates positive staining. Elastic fibers were visualized using Alexa Fluor 633 hydrazide. Scale bar=50 µm. Arrows indicate the position of the IEL. *Neointima.

(*Eln$^{f/f}$* or *Eln$^{f/+}$*), had developed substantial neointima (Figure 2B). These results show that migration of SMCs into the intimal space occurs postnatally and that the integrity of the IEL is a mitigating factor.

Secondary Heart Field-Derived SMCs Are Significant Contributors to Neointima

Previous studies established that cells in the inner portion of the mouse ascending aorta are mostly from the cardiac neural crest (NC), whereas cells with a secondary heart field (SHF) lineage populate the outer part of the

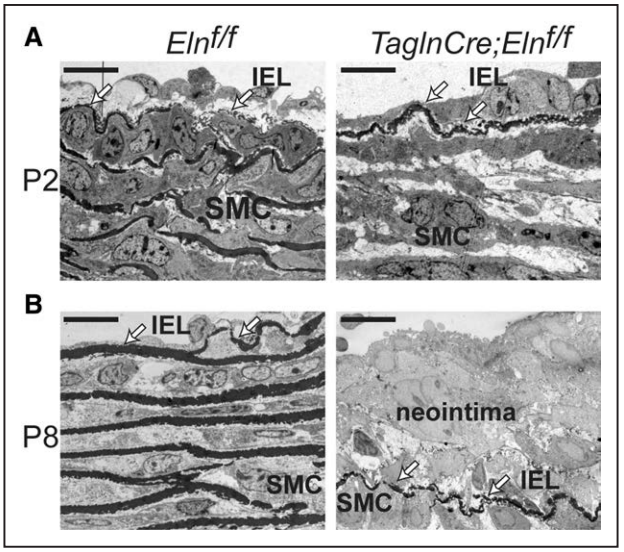

Figure 2. Neointima in the *TagInCre;Eln$^{f/f}$* ascending aorta develops shortly after birth.
A, Transmission electron micrographs show a discontinuous internal elastic lamina (IEL, arrows) in both control and *TagInCre;Eln$^{f/f}$* ascending aorta shortly after birth (P2). Neointima is not evident in either artery. **B**, At P8, the IEL (arrows) is complete in the control aorta but remains discontinuous in *TagInCre;Eln$^{f/f}$* ascending aorta where substantial neointima is evident. Scale bars=10 μm. SMC indicates smooth muscle cells.

wall.[18] We took advantage of *Cre* drivers known to target these aortic SMC subsets to identify how each might contribute to neointima formation. To genetically fate-map and inactivate Eln production in SHF-derived cells, *Eln$^{f/f}$* mice were crossed with mice bearing the *Isl1Cre* transgene, which is expressed in SHF cells.[8] *Isl1Cre;Eln$^{f/f}$* mice were born at the expected Mendelian frequency (observed/expected =27/27.25, *P*=0.96), were fertile, and grossly resembled *Eln$^{f/+}$* animals (Figure 3A). Survival analysis showed that about 25% of the *Isl1Cre;Eln$^{f/f}$* animals died before weaning, with ≈50% alive beyond 4 months of age (n=26 *Isl1Cre;Eln$^{f/f}$* mice; Figure 3B).

Lineage tracing with the *ROSA26$^{mT/mG}$* reporter confirmed recombination in SMCs in the outer portion of the *Isl1Cre;Eln$^{f/+}$* ascending aorta and in ECs (Figure 3C). Histological staining for elastic fibers confirmed the absence of Eln in the SHF region. Elastic lamellae in the inner area populated by NC-derived cells were present but not always intact (Figure 3D). As with the *TagInCre;Eln$^{f/f}$* mice described above, neointimal hyperplasia occurred in the majority of *Isl1Cre;Eln$^{f/f}$* animals and was particularly prominent around breaches in the IEL (Figure 3D). Lineage tracing using the *ROSA26$^{mT/mG}$* reporter showed that most neointimal cells were green, implying a SHF lineage (Figure 3E). Eln-producing cells (red, non-*Isl1Cre* lineage) were in the media and colocalized with elastic fibers, although a small number of red cells were found within the neointima (Figure 3E). These results show that neointimal cells in the ascending aorta of *Isl1Cre;Eln$^{f/f}$* mice are predominantly of SHF origin.

Loss of Eln in NC-Derived SMCs Causes Wall Thickening, Premature Death, and Sporadic Neointima

SMCs populating the inner portion of the ascending aorta originate from the cardiac NC. To explore how these cells contribute to vessel wall remodeling and neointima formation, we crossed *Eln$^{f/f}$* mice with mice bearing the *Wnt1Cre* transgene, which is expressed in NC cells. *Wnt1Cre;Eln$^{f/f}$* mice were appreciably smaller than control littermates within the first week after birth (Figure 4A) and showed a high degree of perinatal lethality (Mendelian frequency, observed/expected 28/45, *P*=0.0034 between P5 and P13). Most died at 1 to 2 weeks of age, although some survived up to 2 to 3 months. Using the *ROSA26$^{mT/mG}$* reporter, we documented that recombination occurred predominantly in the inner aortic wall area, although some intermixing with SHF cells was observed (Figure 4B).

Histology of *Wnt1Cre;Eln$^{f/f}$* ascending aorta found relatively intact elastic layers in the outer section of the ascending aorta (SHF region) and fragmented elastic fibers scattered in the inner layers (NC region; Figure 4C). There was extensive medial expansion in the region of the wall where Eln was absent. Among the *Wnt1Cre;Eln$^{f/f}$* ascending aortas evaluated with histology at P6 or older, in two-thirds (8/12), the IEL remained relatively intact, and neointima was not detected, even in the few animals that lived for several months (Figure 4D). In the other one-third, 2 to 3 layers of intimal cells were observed (Figure 4E through 4G). The *ROSA26$^{mT/mG}$* reporter demonstrated that at P6, most of the neointimal cells arose from the *Wnt1Cre* lineage, although many non-NC-derived cells were observed (Figure 4F). At 2.5 months of age, the neointimal burden in *Wnt1Cre;Eln$^{f/f}$* ascending aorta, when present, remained substantially lower than that of *Isl1Cre;Eln$^{f/f}$* ascending aorta (Figure 4G). Therefore, both aortic SHF- and NC-derived SMCs can contribute to neointima.

Aortic Arch Coarctation Occurs in *TagInCre;Eln$^{f/f}$* and *Wnt1Cre;Eln$^{f/f}$*, but Not *Isl1Cre;Eln$^{f/f}$* Animals

Latex angiography identified a severe coarctation of the *Wnt1Cre;Eln$^{f/f}$* aortic arch (Figure 4H), similar to that found in *TagInCre;Eln$^{f/f}$* animals.[5] The location of the coarctation (at or distal to the brachiocephalic artery branch) and the timing of its formation were similar in both genotypes. Histological analysis showed that combined medial hyperplasia and neointimal formation were responsible for obstructive lesion formation in *TagInCre;Eln$^{f/f}$* animals, whereas medial hyperplasia was the primary mode of obstruction in *Wnt1Cre;Eln$^{f/f}$* aortic arch (Figure I in the

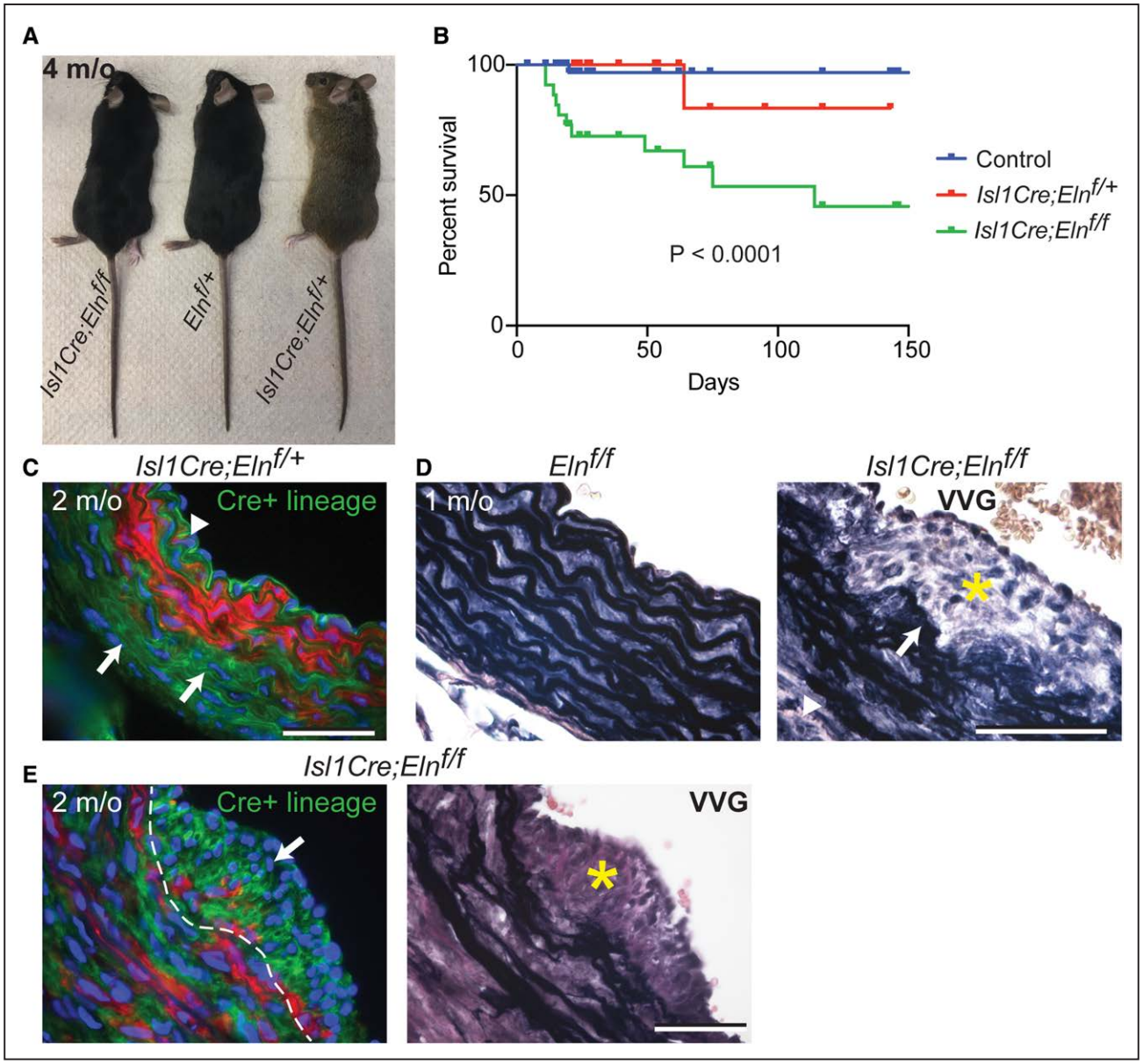

Figure 3. Secondary heart field-derived cells contribute to neointima.
A, Four-month-old *Isl1Cre;Eln*$^{f/f}$ animals grossly resembled littermate controls. **B**, Survival curve of *Isl1Cre;Eln*$^{f/f}$ animals compared with *Isl1Cre;Eln*$^{f/+}$ and controls (both *Eln*$^{f/+}$ and *Eln*$^{f/f}$). $P<0.0001$ for comparing all curves, or *Isl1Cre;Eln*$^{f/f}$ vs controls. **C**, The *ROSA26*$^{mT/mG}$ lineage-tracing allele showed *Isl1Cre*-mediated recombination in smooth muscle cells (SMCs) in the outer portion of the ascending aorta (arrows), as well as in endothelial cells and a small number of SMCs close to the internal elastic lamina (IEL; arrowhead). **D**, Verhoeff-van Gieson (VVG)-stained aortic section showing the absence of elastic fibers in the outer region of *Isl1Cre;Eln*$^{f/f}$ ascending aorta (arrowhead) and present in the inner region (arrow) of the wall. The yellow asterisk marks the neointima. **E**, The *ROSA26*$^{mT/mG}$ allele shows that neointimal cells (arrow) are mostly derived from the *Isl1Cre*-lineage (green). The position of the IEL is indicated by a dashed line based on the brightfield VVG image (**right**) from the same section. Scale bars=50 μm.

Data Supplement). No aortic arch malformations were observed in *Isl1Cre;Eln*$^{f/f}$ mice.

A SHF Cell-Derived Population Adjacent to the IEL

An unexpected finding from the lineage-tracing studies was the presence of a small population of *Isl1*-positive (SHF) cells underneath and adjacent to the IEL in *Isl1Cre;Eln*$^{f/+}$;*ROSA26*$^{mT/mG}$ ascending aorta (Figure 3C). A similar number of non-NC sub-IEL cells (red cells) were also evident with the *Wnt1Cre;Eln*$^{f/+}$;*ROSA26*$^{mT/mG}$ reporter. While it was not possible to directly confirm that these *Wnt1Cre*-negative cells were of SHF lineage, their abundance and location corresponded to the SHF cells observed with the *Isl1Cre;Eln*$^{f/+}$;*ROSA26*$^{mT/mG}$ reporter. As mentioned above, the *Isl1Cre* lineage gives rise to both ECs and SMCs (Figure 3C). To

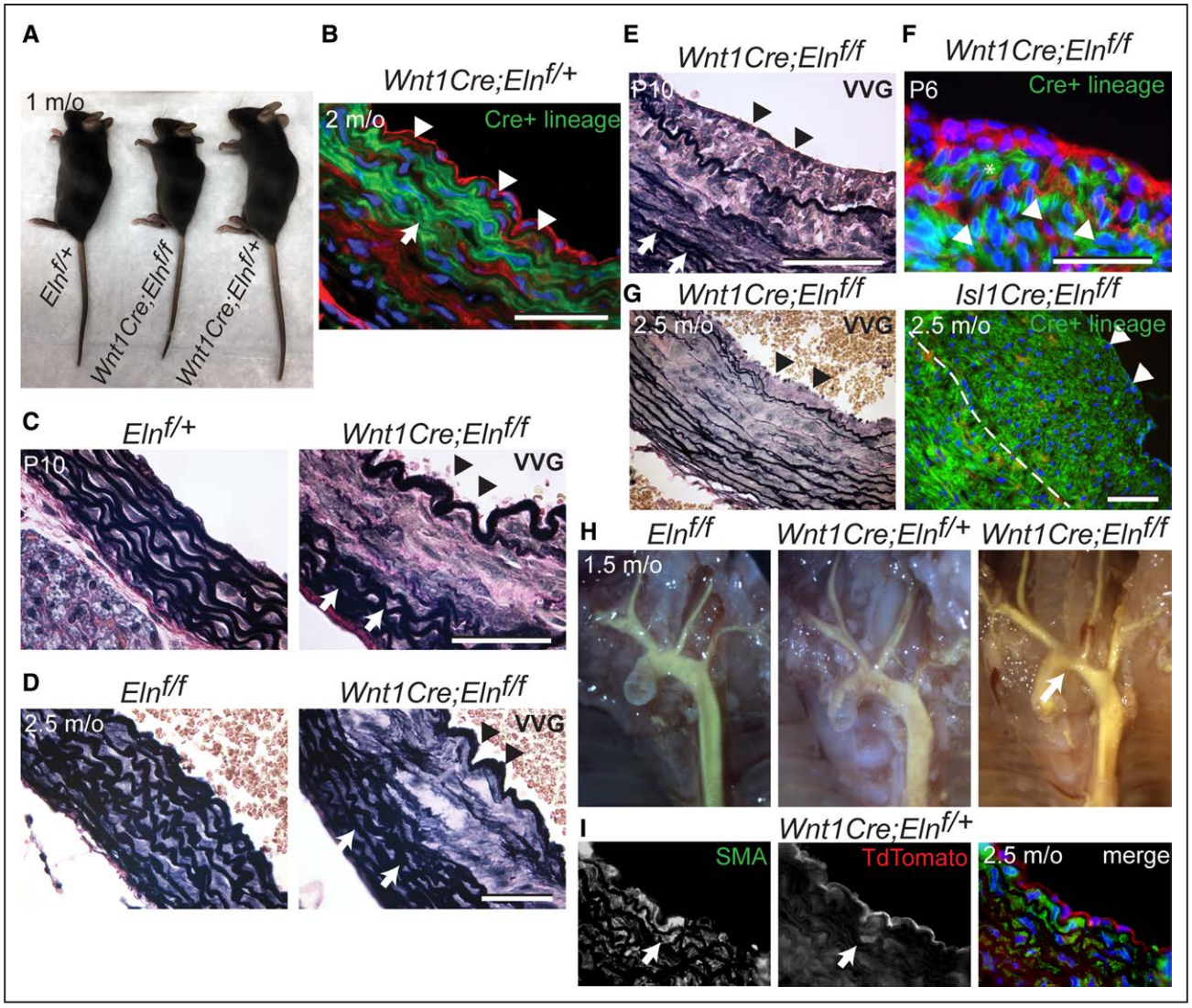

Figure 4. Elastin deletion in neural crest-derived cells results in neointima and aortic coarctation.
A, One-month-old *Wnt1Cre;Eln*$^{f/f}$ animals were smaller compared with littermate controls. **B**, The *ROSA26*$^{mT/mG}$ lineage-tracing allele in a 2-mo-old *Wnt1Cre;Eln*$^{f/+}$ mouse showed *Wnt1Cre*-mediated recombination in smooth muscle cells (SMCs) in the inner portion of the ascending aorta (arrow). Note the nonrecombined cells, likely from secondary heart field (SHF) lineage, adjacent to the internal elastic lamina (IEL; arrowheads). **C** and **D**, Verhoeff-van Gieson (VVG) staining shows an intact IEL (black arrowhead) and no neointima in P10 (**C**) and 2.5-mo-old (**D**) *Wnt1Cre;Eln*$^{f/f}$ ascending aorta. White arrows indicate elastic layers made by SHF-derived SMC in the outer region. **E**, Neointima does occur in a small number of animals. Shown is a VVG stain of a P10 *Wnt1Cre;Eln*$^{f/f}$ ascending aorta. Black arrowheads mark the neointima and white arrows indicate elastic layers made by SHF-derived SMC in the outer region. **F**, The *ROSA26*$^{mT/mG}$ allele showed that most neointimal cells originated from the neural crest (NC) lineage in a P6 *Wnt1Cre;Eln*$^{f/f}$ ascending aorta. White arrowheads indicate the IEL, which is visualized with Alexa Fluor 633 hydrazide. **G**, VVG staining shows less neointimal burden (arrowheads) in the ascending aorta of a 2.5-mo-old *Wnt1Cre;Eln*$^{f/f}$ mouse compared to a *Isl11Cre;Eln*$^{f/f}$ mouse of the same age. The IEL is indicated by a dashed line. **H**, Coarctation (arrow) seen in 1.5-mo-old *Wnt1Cre;Eln*$^{f/f}$ aortic arch. **I**, Immunostaining of SMA (green) and TdTomato (red) from the *ROSA26*$^{mT/mG}$ lineage-tracing allele in a 2.5-mo-old *Wnt1Cre;Eln*$^{f/+}$ mouse identifies nonrecombined SMCs, likely from the SHF lineage, underneath the IEL in the inner portion of the ascending aorta (arrow). Scale bars=50 μm.

confirm that these non-NC, sub-IEL cells were SMCs, we used an antigen retrieval method on paraffin-embedded *Wnt1Cre*;*Eln*$^{f/+}$;*ROSA26*$^{mT/mG}$ tissue samples to extinguish fluorescence from the EGFP and TdTomato reporters. The samples were then coimmunostained with an antibody to TdTomato protein to identify only non-NC lineage cells and an antibody to smooth muscle actin to mark SMCs. Colocalization of these antibodies confirmed that the sub-IEL non-NC cells were SMCs (Figure 4I).

Single-Cell Transcriptome Analysis Identifies Distinct Cell Populations in the Ascending Aorta

The cellular heterogeneity suggested by the lineage-tracing results raised the likelihood of variability in SMC

phenotypes associated with Eln insufficiency. We used scRNA-seq in the *TagInCre;Eln*$^{f/f}$ mice to explore this possibility. Our goals were 3-fold: (1) To determine how the absence of Eln influences SMC phenotypes; (2) To detect and characterize cellular heterogeneity within the aortic SMC population; and (3) To determine if neointimal SMCs are transcriptionally different from their mural cell counterparts.

Disassociated cells from a pool of 4 P8 *TagInCre;Eln*$^{f/f}$ and 3 control ascending aorta underwent FACS sorting with gating for singlets and using DAPI as a viability indicator (Figure IIA and IIB in the Data Supplement). The single live cells were subjected to the 10× Chromium 3'V3 platform for RNA isolation and library preparation, followed by sequencing using an Illumina NovaSeq sequencer. The raw reads were processed into an expression matrix using CellRanger software, and the Seurat 4 software package[13] was used for analysis and clustering. After quality control, 1860 cells were included in the analysis for *TagInCre;Eln*$^{f/f}$ ascending aorta with an average of 3470 genes and 15 685 unique molecular identifiers per cell (Figure IIC in the Data Supplement). A parallel sequencing run of control ascending aorta contained 579 cells after quality control with an average of 3624 genes and 16 256 unique molecular identifiers per cell (Figure IIC in the Data Supplement).

Unsupervised clustering of the integrated data set (Figure 5A) identified 14 cell clusters (Figure 5B and Figure IID in the Data Supplement). Figure III in the Data Supplement shows the top 5 enriched genes in each cluster. Cell cluster identity was assigned using the highly expressed lineage-specific marker genes within each cluster (Figure 5C). Three clusters are SMC-like and express *Myh11*, *Acta2,* and *Cnn1*. They are hereafter referred to as SMC1, SMC2, and SMC3, respectively. Other cluster assignments include myofibroblasts (*Wisp1*, *Podn*, *Col1a1*, and *Col3a1*), Sca1 progenitor cells (*Ly6a* and *Clec3b*), NC cells (*Npy* and *Tbx20*), macrophages (*C1qc, Pf4*, and *Ccl2*), monocytes (*Ccr2*, *Cybb*, and *Il1b*), 2 groups of T cells (*Cd3g, Cd8b*, and *Trbc2*), B cells (*Igkc, Cd79a*, and *Ms4a*), neutrophils (*S100a8, S100a9*, and *Stfa21*), ECs (*Cdh5, Cldn5*, and *Pecam1*), and glial cells (*Sox10, Mal,* and *Prnp*). Hierarchical clustering analysis supports cluster identification (Figure 5D). Differential proportion analysis[15] shows a higher percentage of NC cells (P=0.013) in control ascending aorta and of monocytes (P=0.026) in *TagInCre;Eln*$^{f/f}$ ascending aorta (Figure 5E). Principal component analyses of enriched pathways show the relationships between clusters (Figure IV in the Data Supplement). Reactome pathway analysis[17] of each cluster's enriched genes highlighted the most significantly enriched pathways for each cell type (Figure V in the Data Supplement). Hence, our scRNA-seq analysis pipeline identifies known cell populations in the P8 mouse aorta. The results highlight the differential distribution of cell types in the *TagInCre;Eln*$^{f/f}$ ascending aorta compared with control, and the diversity of SMC types in both control and *TagInCre;Eln*$^{f/f}$ ascending aorta.

Single-Cell Sequencing Identifies Transcriptional Landscape in Neointima

Because cells in the neointima of *TagInCre;Eln*$^{f/f}$ ascending aorta express SMC markers, we further explored the transcriptional landscape of the 3 different SMC clusters. Figure 5C and Figure III in the Data Supplement show that SMC1 has the highest expression of SMC marker genes. SMC2 has the lowest expression of SMC marker genes and elevated expression of myofibroblast marker genes. SMC3 has an intermediate level of SMC and myofibroblast marker genes. SMC3 also has a high expression of genes associated with cell proliferation, including *Top2a*, *Stmn1*, and *Birc5*. Hierarchical cluster analysis of the expression data found that SMC2 and SMC3 are more transcriptionally like each other than they are to SMC1 (Figure 5D). Reactome gene set enrichment pathway analysis[16] showed that SMC2 and SMC3 lie midway between myofibroblasts/Sca1 and SMC1 clusters along principal component one (Figure IV in the Data Supplement).

Reactome pathway analysis[17] highlights the upregulated pathways for each SMC cluster compared with all other clusters (Figure V in the Data Supplement). SMC1 and SMC2 showed upregulation of extracellular matrix organization, elastic fiber formation, molecules associated with elastic fibers, and collagen formation within the 5 most significant upregulated pathways. However, nonintegrin membrane extracellular matrix interactions rounded out the top 5 for SMC1, while collagen biosynthesis and modifying enzymes were in the top 5 for SMC2. Collagen biosynthesis and modifying enzymes were in the top 5 upregulated pathways for the myofibroblast, Sca1, and NC clusters. All of the top 5 most significant upregulated pathways for SMC3 are related to the cell cycle. Based on the gene expression and pathway analysis, we identify SMC1 as the foremost differentiated SMC cluster in the P8 aortic wall and SMC2 and SMC3 as minor less differentiated clusters.

Transcriptional Profile of SMC2 and SMC3

We subsequently examined the transcriptional differences between SMC2 and SMC3 compared with SMC1. Figure 6A shows the differentially regulated genes, and Figure 6B shows the 5 most significant differentially regulated Reactome pathways in SMC2 and SMC3 compared with SMC1 for the integrated data set. Figure 6A and 6B support the less contractile phenotype of both clusters compared with SMC1, as well as the more fibroblastic, extracellular matrix-producing phenotype of SMC2 and the proliferative phenotype of SMC3. Figure 6C shows expression levels of differentially regulated

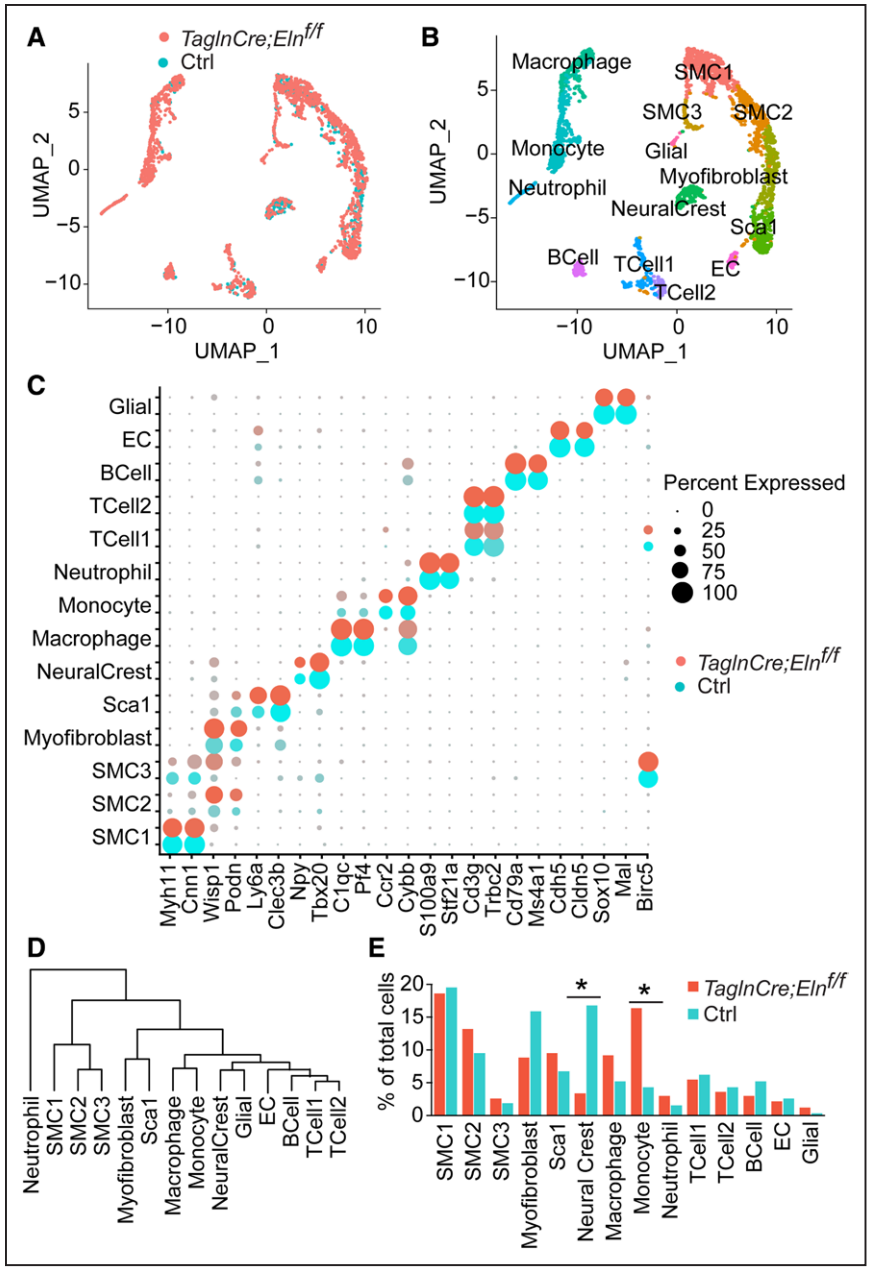

Figure 5. Single-cell RNA sequencing reveals 14 cell populations in *TagInCre;Eln$^{f/f}$* and control P8 ascending aorta.
A, *TagInCre;Eln$^{f/f}$* and control (Ctrl) clusters displayed on UMAP projections. **B**, Integrated clusters with cell identities displayed on UMAP projections. **C**, Dot plot illustrates select genes enriched in each cluster. **D**, Hierarchical clustering analysis of integrated cell clusters. **E**, Percentage of cells in each cluster by genotype. *$P<0.05$.

genes of interest by cluster and genotype. The proliferative gene expression signature is unique to SMC3 for the SMC clusters but is also observed in the TCell1 cluster (Figure 6C and Figure III in the Data Supplement). Immunostaining for Birc5 protein identifies a subset of neointimal cells in *TagInCre;Eln$^{f/f}$* ascending aorta (Figure 6D), suggesting that the small, proliferative SMC3 population is localized to the neointimal region.

Guided by previous studies that implicate hedgehog and notch signaling in neointima formation,[19–22] we focused on identifying the expression of components of these signaling pathways as markers of neointimal cells in *TagInCre;Eln$^{f/f}$* ascending aorta. Analysis of the single-cell sequencing data found that the expression of Notch pathway genes (*Notch1-4*, *Dll1*, and *Jag1*) was similar in all SMC populations (SMC1-3), except for Notch1 that showed elevated but not statistically significant differential expression in SMC3 (Figure VIA in the Data Supplement). In contrast, the hedgehog receptor, Patched (*Ptch1*), was expressed by SMC2 and SMC3, but not SMC1 (Figure 6C). Immunostaining for Patched protein identified positive cells in the control aorta's adventitia (Figure 6E), consistent with previous reports.[20] In *TagInCre;Eln$^{f/f}$* ascending aorta, robust Patched staining was found in neointimal cells but not in SMCs in the media (Figure 6E), thereby localizing SMC2 and SMC3 to the neointimal region. Other components of the hedgehog signaling pathway were not detected (*Shh* and *Dhh*) or were not different (*Ihh*, *Smo*, and *Gli1*) among SMC1-3 (Figure VIB in the Data Supplement). The immunohistochemistry and transcriptomic data show that distinct SMC types are present in both control and

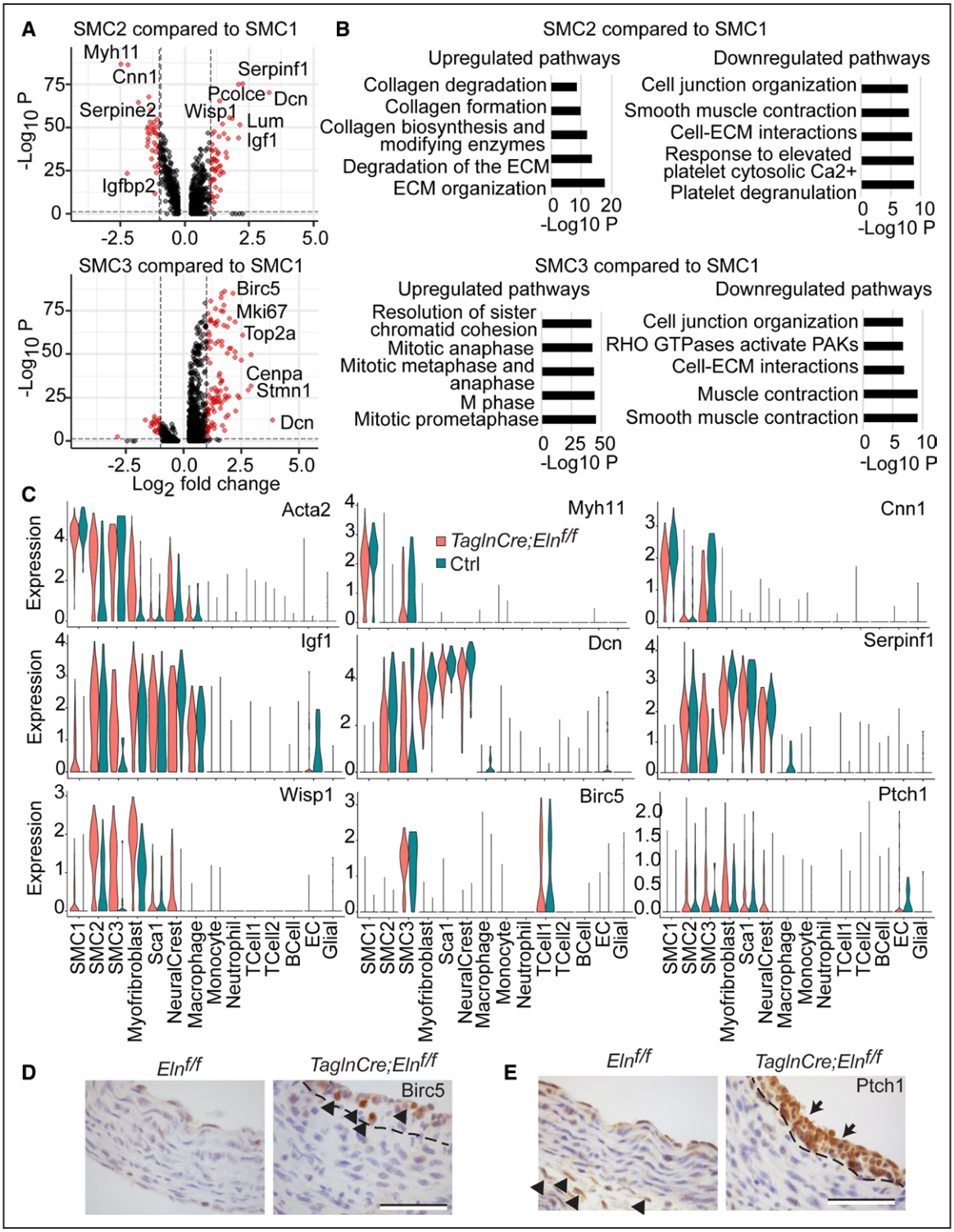

Figure 6. Transcriptional differences and neointimal localization of smooth muscle cell (SMC)2 and SMC3.
A, Volcano plots indicating the most differentially expressed genes between SMC2 (**top**) and SMC3 (**bottom**) compared with SMC1 using the integrated data set. Red points indicate genes with a minimum log2-fold change threshold of 1 and $P<0.05$. **B**, Barplots showing the top 5 most significant upregulated (**left**) and downregulated (**right**) reactome pathways for SMC2 (**top**) and SMC3 (**bottom**) compared with SMC1 in the integrated data set. **C**, Violin plots show expression levels for SMC marker genes (*Acta2*, *Myh11*, and *Cnn1*), some commonly upregulated genes in both SMC2 and SMC3 compared with SMC1 (*Igf1*, *Dcn*, and *Serpinf1*), myofibroblast marker genes (*Wisp1*), proliferation marker genes (*Birc5*), and the hedgehog receptor gene *Ptch1*. **D**, Immunostaining showed Birc5-expressing cells in the neointima in P9 *TagInCre;Eln$^{f/f}$* ascending aorta (arrowheads). Dashed lines indicate internal elastic lamina (IEL). **E**, Immunostaining revealed Ptch1 staining in the neointima in P9 *TagInCre;Eln$^{f/f}$* ascending aorta (arrows). Note the staining in *Eln$^{f/f}$* adventitia (arrowheads). IEL indicated by the dashed lines. The external elastic lamina is outside of the imaged fields in *TagInCre;Eln$^{f/f}$* images, Scale bars=50 μm. ECM indicates extracellular matrix.

diseased aorta and that SMC2 and SMC3 localize to the neointimal region in *TaglnCre;Eln*$^{f/f}$ ascending aorta.

Transcriptional Changes in SMCs due to Eln Deficiency

To determine whether individual SMC populations in *TaglnCre;Eln*$^{f/f}$ were transcriptionally distinct from those in the control aorta, we compared expression between genotypes for each SMC cluster. There were 147 upregulated and 184 downregulated genes in SMC1 *TaglnCre;Eln*$^{f/f}$ ascending aorta compared with control (Table II in the Data Supplement and Figure 7A). The most highly upregulated gene in the mutant aorta was *Igfbp2*, which was also the highest upregulated gene found in our previous microarray experiment comparing global *Eln* knockout versus control aorta.[23] Reactome pathway analysis shows that the regulation of IGF transport and uptake by IGFBPs is the second most significantly upregulated pathway (Figure 7B). *Igfbp2* is upregulated specifically in *TaglnCre;Eln*$^{f/f}$ SMC clusters (Figure 7C), and immunostaining shows Igfbp2 protein throughout the *TaglnCre;Eln*$^{f/f}$ aorta, indicating expression by all SMCs (Figure 7D). Immunostaining of human coronary artery neointimal tissues from cardiac allograft vasculopathy showed that most cells in the neointima stained positive for IGFBP2 (Figure 7E). In contrast, the staining signal was absent in the normal coronary artery from an autopsy sample or a negative control stained without a primary antibody (Figure VII in the Data Supplement).

The most downregulated gene in SMC1 *TaglnCre;Eln*$^{f/f}$ ascending aorta compared with control was *Pi15* (Figure 7A and 7C), which was also downregulated when comparing global *Eln* knockout versus control aorta.[23] Nine of the 25 differentially regulated genes (*Pi15, Igfbp2, Itgbl1, Wnt16, Gna14, Ltbp2, Adamts8, Thbs1*, and *Ctgf*) in our previous microarray analysis were found differentially regulated in SMC1 of *TaglnCre;Eln*$^{f/f}$ ascending aorta compared with control, validating this computational approach. Additional genes upregulated in SMC1 include *Wisp2* (also known as *Ccn5*), a matricellular gene that inhibits SMC proliferation,[24] *Fn1*, a cell adhesion molecule,[25] and *Fbln2*, and *Fbln5,* extracellular matrix genes associated with elastic fiber assembly (Figure 7C).[26] Reactome pathway analysis indicates upregulation of matrix organization and elastic fiber formation in *TaglnCre;Eln*$^{f/f}$ ascending aorta compared with control (Figure 7B). These results show that the absence of Eln alters the transcriptional signature of SMC1, the predominant SMC type in the aortic wall.

Ninety-four genes were upregulated, and 26 were downregulated in SMC2 *TaglnCre;Eln*$^{f/f}$ ascending aorta compared with control (Table II in the Data Supplement and Figure 7A). Forty-five differentially up or downregulated genes were the same in SMC1 and SMC2, indicating a common SMC response to Eln deficiency. Two of the genes (*Acta2* and *Postn*) were differentially regulated in SMC1 and SMC2 but in opposite directions (Table II in the Data Supplement). The highest upregulated gene in SMC2 *TaglnCre;Eln*$^{f/f}$ ascending aorta compared with control was *Nov*, a matricellular gene also known as *Ccn3* (Figure 7A and 7C). The most downregulated gene was *Apoe* (Figure 7A). Common differentially regulated genes in SMC2 and our previous data on the global *Eln* knockout include *Pi15*, *Itgbl1*, *Ltbp2*, and *Ctgf* (similar to SMC1 above), and *Col8a1*,[23] which was not differentially regulated in SMC1 (Figure 7C). There were no significantly differentially regulated genes in SMC3 *TaglnCre;Eln*$^{f/f}$ ascending aorta compared with control, likely due to the low number of cells in this cluster (Figure IID in the Data Supplement). Overall, these results show commonalities and differences in the response of unique SMC clusters to Eln insufficiency.

DISCUSSION

A characteristic of mice and humans with loss-of-function Eln gene mutations is neointima formation in elastic vessels. In the Eln germ-line knockout mouse with no Eln in the vessel wall, medial SMCs migrate into the lumen, proliferate, and eventually occlude blood flow shortly after birth.[27] When *Eln* is inactivated only in SMCs (*TaglnCre;Eln*$^{f/f}$), an IEL made by ECs serves as an effective barrier to inward cell movement, but neointima still forms where there are breaks in the lamellar structure.[5] These 2 mouse models highlight the importance of Eln in maintaining vessel wall continuity and suggest a role for Eln in influencing SMC phenotypes. Lineage tracing using *TaglnCre;Eln*$^{f/f}$ mice bred into the *ROSA26*$^{mT/mG}$ background established that cells in the neointima are predominantly of SMC origin, a finding in agreement with observations reported by others.[28,29]

Cellular Heterogeneity and SMC Subpopulations

SMCs in the ascending aorta have different embryological origins and a unique distribution, with cells derived from the SHF populating the wall's outer region and NC-derived cells localized near the lumen.[18,30] When SHF- (*Isl1*) and NC- (*Wnt1*) targeted *Cre* drivers were used to lineage mark and inactive Eln in those specific cell populations, we found that mice missing Eln in the SHF (*Isl1Cre*, outer) region of the wall tended to survive into adulthood. That the ascending aorta in these mice serves as a functional conduit vessel with Eln missing from the outer half of the aortic wall is, indeed, surprising. Why some of these animals die before weaning is unclear, but the cause of death most likely relates to a severe emphysema-like phenotype in the lungs of animals that die early (data not shown).

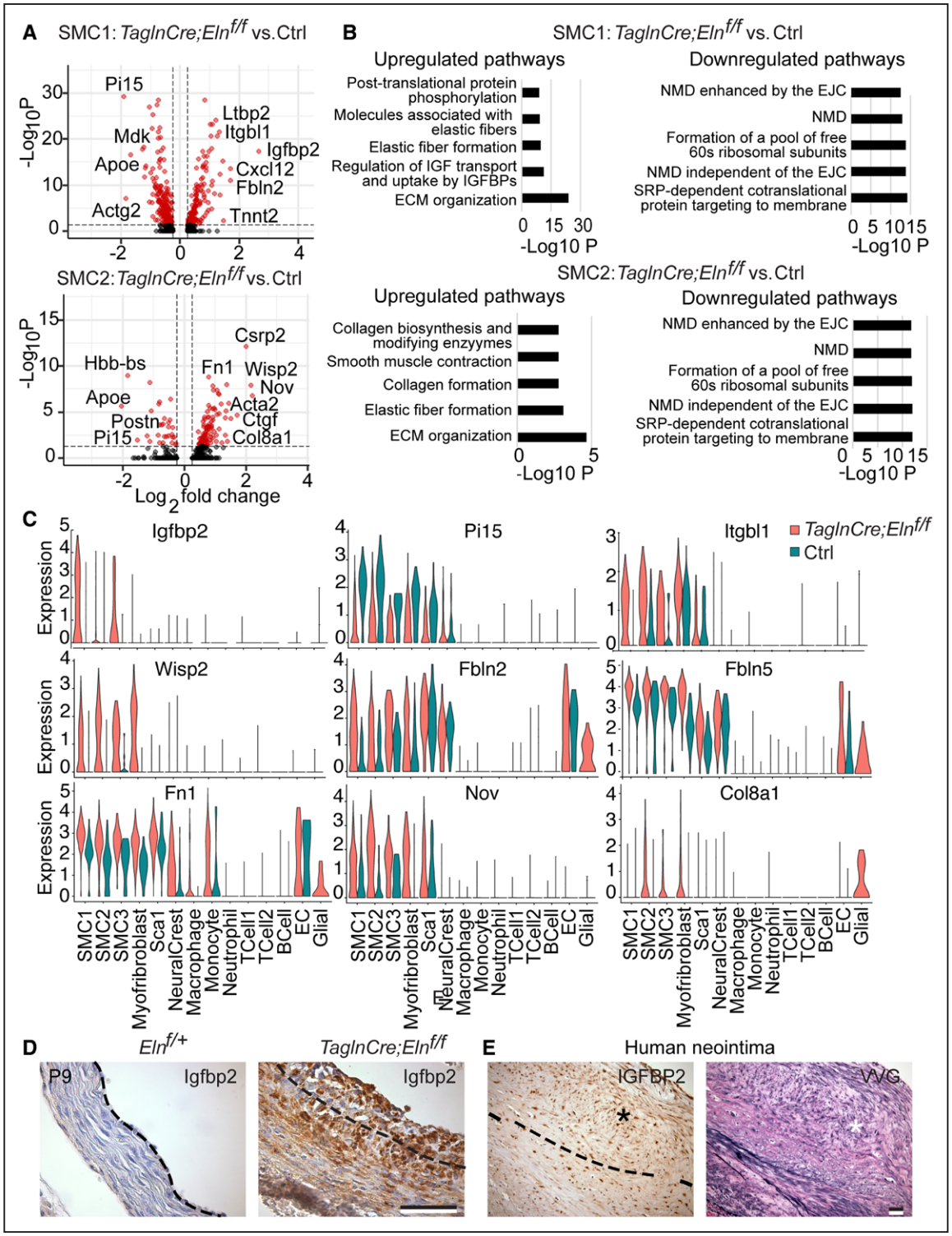

Figure 7. Transcriptional differences in smooth muscle cell (SMC) clusters between *TagInCre;Eln$^{f/f}$* and control ascending aorta. **A**, Volcano plots indicating the most differentially expressed genes between *TagInCre;Eln$^{f/f}$* and control ascending aorta for SMC1 (**top**) and SMC2 (**bottom**). Red points indicate genes with a minimum log2-fold change threshold of 0.25 and $P<0.05$. There are no significant differentially expressed genes between genotypes for the SMC3 cluster. **B**, Barplots showing the top 5 most significant upregulated (**left**) and downregulated (**right**) reactome pathways between *TagInCre;Eln$^{f/f}$* and control ascending aorta for SMC1 (**top**) and SMC2 (**bottom**) in the integrated data set. **C**, Violin plots show expression levels for differentially expressed genes of interest by cluster and genotype. **D**, Immunostaining showed Igfbp2 (insulin-like growth factor-binding protein-2)-expressing cells throughout the wall of P9 *TagInCre;Eln$^{f/f}$* ascending aorta but no expression in control aorta. **E**, Immunostaining (**left**) showed IGFBP2-expressing cells in human coronary artery neointima in a patient with cardiac allograft vasculopathy. Verhoeff-van Gieson (VVG) staining of adjacent section (**right**) was used to visualize the disrupted internal elastic lamina (IEL; dashed lines). Scale bars=50 μm. DVL indicates Disheveled; EJC, exon junction complex; NMD, nonsense-mediated decay; and SRP, signal recognition particle.

Mice with Eln deleted in NC cells (inner part of the wall) show a noticeably different phenotype. In many ways, the phenotype resembles that seen in *TagInCre;Eln$^{f/f}$* mice. Although there was a relatively intact Eln network produced by SHF SMCs in the wall's outer region, *Wnt1Cre;Eln$^{f/f}$* mice, with a few exceptions, did not survive >2 weeks. The animals were smaller than their wild-type littermates and developed the same aortic arch coarctation found in *Tagln*Cre*;Eln$^{f/f}$* animals. Their exact cause of death is unknown, although cardiac hypertrophy points to heart problems associated with aortic stenosis similar to that found in *TagInCre;Eln$^{f/f}$* animals.[5]

To explore how the absence of Eln influences vascular cell phenotypes, we used scRNA-seq technology to identify transcriptional differences between cells in the aortic wall of wild-type and Eln-deficient mice. In addition to the heterogeneity related to developmental lineage (NC and SHF derived), our study identified 3 SMC subgroups (SMC1, SMC2, and SMC3) present in both *Tagln*Cre*;Eln$^{f/f}$*, and control aorta. This cellular heterogeneity is consistent with evidence from other studies supporting SMC cellular subpopulations within the media of the normal vascular wall.[31] Unsupervised clustering of the transcriptional signatures along with hierarchical clustering analyses showed that SMC2 and SMC3 are dissimilar from the majority of SMCs (SMC1) in *Tagln*Cre*;Eln$^{f/f}$* and control aorta and are themselves unique cell populations. For example, the common expression of SMC cytoskeletal genes confirmed their SMC lineage, but the expression of *Myh11* and *Cnn1* was higher in SMC3 compared with SMC2 (Figure 6C). There was little overlap between most top differentially regulated genes or upregulated reactome pathways in SMC2 and SMC3 compared with SMC1 (Figure 6A). However, 4 out of 5 of the downregulated pathways did overlap (Figure 6B). Only SMC3 showed an increase in genes and reactome pathways associated with cell proliferation. The genes and pathways upregulated in the SMC2 and SMC3 populations are also highly expressed in the myofibroblast, Sca1, and NC cell clusters (Figures III, IV, and V in the Data Supplement), suggesting a connection between these cell types.

Eln Insufficiency and Cellular Phenotypes

RNA-seq analysis showed significant transcriptional changes within the SMC subgroups in response to Eln insufficiency. SMC1, the main differentiated subgroup populating the medial layer, showed increases in molecules and pathways associated with elastic fiber formation in *Tagln*Cre*;Eln$^{f/f}$* compared with control aorta. These changes indicate a compensatory response that was not observed in bulk, ascending aortic gene array for the germ-line Eln knockout mouse,[23] but was observed by in situ hybridization for the developing chick aorta in a model of hemodynamic Eln deficiency.[32] SMC1 cells appear to sense and respond to Eln insufficiency by upregulating elastic fiber synthesis pathways, which is a positive indicator for elastic fiber-associated disease treatments. SMC1 also showed upregulation of molecules and pathways involved in IGF regulation by IGFBPs in *Tagln*Cre*;Eln$^{f/f}$* compared with control aorta. IGF signaling was also implicated in the transcriptional changes in SMC2/3 compared with SMC1.

Eln Insufficiency and Neointima Formation

Both *Isl1Cre;Eln$^{f/f}$* and *Wnt1Cre;Eln$^{f/f}$* mice develop neointima but with interesting differences. The majority of mice with Eln deleted in SHF-derived SMCs and ECs showed neointima throughout the ascending aorta, similar to what was found when Eln was deleted in all SMCs (*Tagln*Cre*;Eln$^{f/f}$*). Lineage tracing using *ROSA26$^{mT/mG}$* established that most cells within the neointima were of *Isl1Cre* lineage. The descending aorta was not affected, consistent with the absence of SHF-derived cells distal to the ascending aorta.[18] Neointima was also observed in the aorta of mice with Eln deleted in NC cells but occurred with lower prevalence (≈1/3 of animals) compared with SHF knockouts. At a similar age, *Wnt1Cre;Eln$^{f/f}$* animals had a smaller neointimal burden than *Isl1Cre;Eln$^{f/f}$* animals. Lineage tracing showed that neointimal cells in *Wnt1Cre;Eln$^{f/f}$* aorta were both NC and SHF in origin. Most of the unrecombined cells, in contrast, remained associated with Eln in the vessel wall, indicating that the presence of Eln either acts as a physical barrier to migration for these cells or down-regulates cell movement and division, as has been suggested by Li et al.[33]

The source of the neointimal SHF cells is an intriguing question. Lineage tracing established that differentiated SMCs in the media contribute to most of the neointimal cells in mouse injury models using arterial wire insertion or carotid ligation.[34] Other studies suggest that some neointimal cells originate from progenitor cell populations in the media[28] or near the medial-adventitial boarder[19,20,35]—the region likely to harbor aortic cells with a SHF lineage. It is unknown if aortic progenitor cells in the adventitial progenitor niche have a SHF origin, but the niche location within or adjacent to the SHF region makes it likely. Majesky et al[29] showed that differentiated SMCs that move into this progenitor niche become reprogrammed to a progenitor-like state and become *Klf4* positive and SMC-marker negative. Because of their location adjacent to the adventitia, SHF-derived cells are the SMCs most likely to undergo this transition in the ascending aorta. If these are the cells that migrate from the progenitor niche into the intima, reprogramming from a SMC-marker negative progenitor cell to a fully differentiated SMC occurs somewhere along the way.

An alternative source for neointimal SHF-derived cells is the medial SMC population directly adjacent to the IEL. In our lineage-tracing experiments, many of

these cells were marked by *Isl1Cre*, suggesting a SHF origin (Figure 3C). These cells are ideally situated to move into the intimal space through breaks in the IEL without traversing the vessel from the outer wall SHF region (graphical abstract). It is interesting that studies using *Mef2c-AHF-Cre*, driven by a different promoter used to lineage mark SHF cells, did not identify this cell population.[18] *Mef2c* is a transcriptional target of *Isl1*, so it is possible that the 2 promoters have different SHF expression profiles, which could account for differential labeling of SHF subpopulations.[36] Identifying individual genes capable of differentiating SHF subpopulations will be required to investigate whether these inner SHF cells are different from their outer wall SHF counterparts and whether these cells might be uniquely primed to clonally expand once in the intima.

Genetic Versus Injury Models

The gene signatures in neointimal cells suggest that some mechanisms underlying neointima formation in Eln insufficiency are common to adult vessel injury models. For example, SMC2 and SMC3 had increased expression of *Igf1* compared with SMC1 (Figure 6A and 6B and Table II in the Data Supplement). Insulin-like growth factor signaling has been implicated in the pathogenesis of neointima, and dominant-negative inhibition of the *Igf1* receptor has been shown to reduce neointima in vascular injury models.[37] Many of the genes most enriched in the neointimal clusters (*Dcn*[38] and *Wisp1*[39] for SMC2 and SMC3, *Ltbp1* for SMC2; *Stmn1*, *Mki67*, *Birc5* for SMC3) have been described previously in studies of neointimal lesions.[40–43] There are, however, some interesting differences in gene expression that indicate unique neointimal cell types. For example, integrin β3 is a protein shown to regulate atherosclerotic plaque cell clonality and fate and is proposed as a therapeutic target for supravalvular aortic stenosis.[44,45] Our single-cell sequencing data showed no differential expression of this or any integrin β chain between the SMC subgroups (Figure VIC in the Data Supplement).

Limitations of the Study

It should be noted that while SMC markers in the neointima support a SMC identity for the neointimal cells, using a constitutively active *TaglnCre* driver makes it impossible to rule out non-SMCs (eg, adventitial cells) adopting a SMC program and expressing *TaglnCre* before becoming a neointimal cell. Likewise, because our SHF lineage tracing uses a constitutive *Cre* (*Isl1Cre*), we cannot distinguish between neointimal cells originating from a differentiated SHF SMC or a Sca1+, SHF-derived progenitor that has undergone phenotypic switching to express a SMC signature. Dynamic labeling of cell lineages using *Isl1*- or *Wnt1*-driven promoters is also not possible since both *Isl1* and *Wnt1* expression are silenced in SMCs shortly after birth. Therefore, neither can be used as a marker either in the single-cell sequencing data set or to retrospectively identify SHF- or NC-derived SMC.

The potential for neointima formation by *Isl1* and *Wnt1* lineage SMCs in the Eln knockout aorta cannot be directly compared because of the complex expression pattern of *Isl1* compared with *Wnt1*. *Isl1*, but not *Wnt1*, recombines in the endothelium. Because ECs contribute Eln to the IEL,[5] their inability to do so in the *Isl1Cre:Eln*$^{f/f}$ vessels may result in greater IEL fragmentation and provide more avenues for cellular egress from the vessel wall into the intima. It is also possible that the SHF SMCs adjacent to the IEL play a role in maintaining IEL integrity, which is prevented with Eln gene inactivation by *Isl1Cre*. It should be noted, however, that no neointima is observed when Eln expression is specifically inactivated in ECs (*Tie2-Cre* or *Cdh5-Cre*).[5]

Conclusions

Neointima formation remains a clinically significant issue despite advances in therapeutic approaches. The current mainstay of therapy against neointimal formation uses drug-eluting stents. These drugs, typically directed towards inhibiting cell proliferation, may target only a subset of neointimal cells (eg, equivalent to SMC3) while leaving other neointimal cells (eg, equivalent to SMC2) unaddressed. Therefore, understanding the phenotypic and functional diversity of neointimal cells may provide additional therapeutic targets and functional approaches for addressing vascular remodeling in the disease setting.

ARTICLE INFORMATION

Received November 21, 2020; accepted September 13, 2021.

Affiliations

Department of Cell Biology and Physiology (C.-J.L., B.M.H., R.A.R., R.P.M.), Cardiovascular Division, Department of Medicine (C.-J.L.), Department of Pathology and Immunology (C.-Y.L.), and Mechanical Engineering and Materials Science (J.E.W.), Washington University School of Medicine, St Louis, MO.

Acknowledgments

We acknowledge assistance from the Histology and Microscopy Core facility in the Department of Developmental Biology, Washington University School of Medicine.

Sources of Funding

This study was partially funded by National Science Foundation grant 1662434 (J.E. Wagenseil) and National Institutes of Health grants R56 HL152420 (J.E. Wagenseil) and HL-53325 (R.P. Mecham). C.-J. Lin was supported by T32HL007081 and T32HL125241. The Ines Mandl Research Foundation also provided funds to R.P. Mecham.

Disclosures

None.

Supplemental Materials

Data Supplement Figures I–VII
Data Supplement Tables I–II

REFERENCES

1. Cox JL, Chiasson DA, Gotlieb AI. Stranger in a strange land: the pathogenesis of saphenous vein graft stenosis with emphasis on structural and functional differences between veins and arteries. *Prog Cardiovasc Dis*. 1991;34:45–68. doi: 10.1016/0033-0620(91)90019-i
2. Motwani JG, Topol EJ. Aortocoronary saphenous vein graft disease: pathogenesis, predisposition, and prevention. *Circulation*. 1998;97:916–931. doi: 10.1161/01.cir.97.9.916
3. Roy-Chaudhury P, Arend L, Zhang J, Krishnamoorthy M, Wang Y, Banerjee R, Samaha A, Munda R. Neointimal hyperplasia in early arteriovenous fistula failure. *Am J Kidney Dis*. 2007;50:782–790. doi: 10.1053/j.ajkd.2007.07.019
4. Urbán Z, Riazi S, Seidl TL, Katahira J, Smoot LB, Chitayat D, Boyd CD, Hinek A. Connection between elastin haploinsufficiency and increased cell proliferation in patients with supravalvular aortic stenosis and Williams-Beuren syndrome. *Am J Hum Genet*. 2002;71:30–44. doi: 10.1086/341035
5. Lin CJ, Staiculescu MC, Hawes JZ, Cocciolone AJ, Hunkins BM, Roth RA, Lin CY, Mecham RP, Wagenseil JE. Heterogeneous cellular contributions to elastic laminae formation in arterial wall development. *Circ Res*. 2019;125:1006–1018. doi: 10.1161/CIRCRESAHA.119.315348
6. Holtwick R, Gotthardt M, Skryabin B, Steinmetz M, Potthast R, Zetsche B, Hammer RE, Herz J, Kuhn M. Smooth muscle-selective deletion of guanylyl cyclase-A prevents the acute but not chronic effects of ANP on blood pressure. *Proc Natl Acad Sci USA*. 2002;99:7142–7147. doi: 10.1073/pnas.102650499
7. Boucher P, Gotthardt M, Li WP, Anderson RG, Herz J. LRP: role in vascular wall integrity and protection from atherosclerosis. *Science*. 2003;300:329–332. doi: 10.1126/science.1082095
8. Cai CL, Liang X, Shi Y, Chu PH, Pfaff SL, Chen J, Evans S. Isl1 identifies a cardiac progenitor population that proliferates prior to differentiation and contributes a majority of cells to the heart. *Dev Cell*. 2003;5:877–889. doi: 10.1016/s1534-5807(03)00363-0
9. Lewis AE, Vasudevan HN, O'Neill AK, Soriano P, Bush JO. The widely used Wnt1-Cre transgene causes developmental phenotypes by ectopic activation of Wnt signaling. *Dev Biol*. 2013;379:229–234. doi: 10.1016/j.ydbio.2013.04.026
10. Muzumdar MD, Tasic B, Miyamichi K, Li L, Luo L. A global double-fluorescent Cre reporter mouse. *Genesis*. 2007;45:593–605. doi: 10.1002/dvg.20335
11. Gallo EM, Loch DC, Habashi JP, Calderon JF, Chen Y, Bedja D, van Erp C, Gerber EE, Parker SJ, Sauls K, et al. Angiotensin II-dependent TGF-β signaling contributes to Loeys-Dietz syndrome vascular pathogenesis. *J Clin Invest*. 2014;124:448–460. doi: 10.1172/JCI69666
12. Kim K, Shim D, Lee JS, Zaitsev K, Williams JW, Kim KW, Jang MY, Seok Jang H, Yun TJ, Lee SH, et al. Transcriptome analysis reveals nonfoamy rather than foamy plaque macrophages are proinflammatory in atherosclerotic murine models. *Circ Res*. 2018;123:1127–1142. doi: 10.1161/CIRCRESAHA.118.312804
13. Stuart T, Butler A, Hoffman P, Hafemeister C, Papalexi E, Mauck WM 3rd, Hao Y, Stoeckius M, Smibert P, Satija R. Comprehensive integration of single-cell data. *Cell*. 2019;177:1888–1902.e21. doi: 10.1016/j.cell.2019.05.031
14. Blighe K, Rana S, Lewis M. EnhancedVolcano: publication-ready volcano plots with enhanced colouring and labeling. *R package version 1.8.0*. 2020. https://github.com/kevinblighe/EnhancedVolcano
15. Farbehi N, Patrick R, Dorison A, Xaymardan M, Janbandhu V, Wystub-Lis K, Ho JW, Nordon RE, Harvey RP. Single-cell expression profiling reveals dynamic flux of cardiac stromal, vascular and immune cells in health and injury. *Elife*. 2019;8:e43882. doi: 10.7554/eLife.43882
16. Griss J, Viteri G, Sidiropoulos K, Nguyen V, Fabregat A, Hermjakob H. ReactomeGSA - efficient multi-omics comparative pathway analysis. *Mol Cell Proteomics*. 2020;19:2115–2125. doi: 10.1074/mcp.TIR120.002155
17. Yu G, He QY. ReactomePA: an R/Bioconductor package for reactome pathway analysis and visualization. *Mol Biosyst*. 2016;12:477–479. doi: 10.1039/c5mb00663e
18. Sawada H, Rateri DL, Moorleghen JJ, Majesky MW, Daugherty A. Smooth muscle cells derived from second heart field and cardiac neural crest reside in spatially distinct domains in the media of the ascending Aorta-brief report. *Arterioscler Thromb Vasc Biol*. 2017;37:1722–1726. doi: 10.1161/ATVBAHA.117.309599
19. Dutzmann J, Koch A, Weisheit S, Sonnenschein K, Korte L, Haertlé M, Thum T, Bauersachs J, Sedding DG, Daniel JM. Sonic hedgehog-dependent activation of adventitial fibroblasts promotes neointima formation. *Cardiovasc Res*. 2017;113:1653–1663. doi: 10.1093/cvr/cvx158
20. Passman JN, Dong XR, Wu SP, Maguire CT, Hogan KA, Bautch VL, Majesky MW. A sonic hedgehog signaling domain in the arterial adventitia supports resident Sca1+ smooth muscle progenitor cells. *Proc Natl Acad Sci USA*. 2008;105:9349–9354. doi: 10.1073/pnas.0711382105
21. Steffes LC, Froistad AA, Andruska A, Boehm M, McGlynn M, Zhang F, Zhang W, Hou D, Tian X, Miquerol L, et al. A Notch3-marked subpopulation of vascular smooth muscle cells is the cell of origin for occlusive pulmonary vascular lesions. *Circulation*. 2020;142:1545–1561. doi: 10.1161/CIRCULATIONAHA.120.045750
22. Tian DY, Jin XR, Zeng X, Wang Y. Notch signaling in endothelial cells: is it the therapeutic target for vascular neointimal hyperplasia? *Int J Mol Sci*. 2017;18:E1615. doi: 10.3390/ijms18081615
23. Staiculescu MC, Cocciolone AJ, Procknow JD, Kim J, Wagenseil JE. Comparative gene array analyses of severe elastic fiber defects in late embryonic and newborn mouse aorta. *Physiol Genomics*. 2018;50:988–1001. doi: 10.1152/physiolgenomics.00080.2018
24. Lake AC, Bialik A, Walsh K, Castellot JJ Jr. CCN5 is a growth arrest-specific gene that regulates smooth muscle cell proliferation and motility. *Am J Pathol*. 2003;162:219–231. doi: 10.1016/S0002-9440(10)63813-8
25. Kumra H, Sabatier L, Hassan A, Sakai T, Mosher DF, Brinckmann J, Reinhardt DP. Roles of fibronectin isoforms in neonatal vascular development and matrix integrity. *PLoS Biol*. 2018;16:e2004812. doi: 10.1371/journal.pbio.2004812
26. Chapman SL, Sicot FX, Davis EC, Huang J, Sasaki T, Chu ML, Yanagisawa H. Fibulin-2 and fibulin-5 cooperatively function to form the internal elastic lamina and protect from vascular injury. *Arterioscler Thromb Vasc Biol*. 2010;30:68–74. doi: 10.1161/ATVBAHA.109.196725
27. Li DY, Brooke B, Davis EC, Mecham RP, Sorensen LK, Boak BB, Eichwald E, Keating MT. Elastin is an essential determinant of arterial morphogenesis. *Nature*. 1998;393:276–280. doi: 10.1038/30522
28. Chappell J, Harman JL, Narasimhan VM, Yu H, Foote K, Simons BD, Bennett MR, Jørgensen HF. Extensive proliferation of a subset of differentiated, yet plastic, medial vascular smooth muscle cells contributes to neointimal formation in mouse injury and atherosclerosis models. *Circ Res*. 2016;119:1313–1323. doi: 10.1161/CIRCRESAHA.116.309799
29. Majesky MW, Horita H, Ostriker A, Lu S, Regan JN, Bagchi A, Dong XR, Poczobutt J, Nemenoff RA, Weiser-Evans MC. Differentiated smooth muscle cells generate a subpopulation of resident vascular progenitor cells in the adventitia regulated by Klf4. *Circ Res*. 2017;120:296–311. doi: 10.1161/CIRCRESAHA.116.309322
30. Leroux-Berger M, Queguiner I, Maciel TT, Ho A, Relaix F, Kempf H. Pathologic calcification of adult vascular smooth muscle cells differs on their crest or mesodermal embryonic origin. *J Bone Miner Res*. 2011;26:1543–1553. doi: 10.1002/jbmr.382
31. Lemire JM, Covin CW, White S, Giachelli CM, Schwartz SM. Characterization of cloned aortic smooth muscle cells from young rats. *Am J Pathol*. 1994;144:1068–1081.
32. Espinosa MG, Taber LA, Wagenseil JE. Reduced embryonic blood flow impacts extracellular matrix deposition in the maturing aorta. *Dev Dyn*. 2018;247:914–923. doi: 10.1002/dvdy.24635
33. Karnik SK, Brooke BS, Bayes-Genis A, Sorensen L, Wythe JD, Schwartz RS, Keating MT, Li DY. A critical role for elastin signaling in vascular morphogenesis and disease. *Development*. 2003;130:411–423. doi: 10.1242/dev.00223
34. Herring BP, Hoggatt AM, Burlak C, Offermanns S. Previously differentiated medial vascular smooth muscle cells contribute to neointima formation following vascular injury. *Vasc Cell*. 2014;6:21. doi: 10.1186/2045-824X-6-21
35. Hu Y, Zhang Z, Torsney E, Afzal AR, Davison F, Metzler B, Xu Q. Abundant progenitor cells in the adventitia contribute to atherosclerosis of vein grafts in ApoE-deficient mice. *J Clin Invest*. 2004;113:1258–1265. doi: 10.1172/JCI19628
36. Dodou E, Verzi MP, Anderson JP, Xu SM, Black BL. Mef2c is a direct transcriptional target of ISL1 and GATA factors in the anterior heart field during mouse embryonic development. *Development*. 2004;131:3931–3942. doi: 10.1242/dev.01256
37. Lim HJ, Park HY, Ko YG, Lee SH, Cho SY, Lee EJ, Jameson JL, Jang Y. Dominant negative insulin-like growth factor-1 receptor inhibits neointimal formation through suppression of vascular smooth muscle cell migration and proliferation, and induction of apoptosis. *Biochem Biophys Res Commun*. 2004;325:1106–1114. doi: 10.1016/j.bbrc.2004.10.175
38. Yamakawa T, Bai HZ, Masuda J, Sawa Y, Shirakura R, Ogata J, Matsuda H. Differential expression of proteoglycans biglycan and decorin during neointima formation after stent implantation in normal and

atherosclerotic rabbit aortas. *Atherosclerosis*. 2000;152:287–297. doi: 10.1016/s0021-9150(99)00475-x
39. Williams H, Mill CA, Monk BA, Hulin-Curtis S, Johnson JL, George SJ. Wnt2 and WISP-1/CCN4 induce intimal thickening via promotion of smooth muscle cell migration. *Arterioscler Thromb Vasc Biol*. 2016;36:1417–1424. doi: 10.1161/ATVBAHA.116.307626
40. Langenickel TH, Olive M, Boehm M, San H, Crook MF, Nabel EG. KIS protects against adverse vascular remodeling by opposing stathmin-mediated VSMC migration in mice. *J Clin Invest*. 2008;118:3848–3859. doi: 10.1172/JCI33206
41. Blanc-Brude OP, Yu J, Simosa H, Conte MS, Sessa WC, Altieri DC. Inhibitor of apoptosis protein survivin regulates vascular injury. *Nat Med*. 2002;8:987–994. doi: 10.1038/nm750
42. Sinha S, Heagerty AM, Shuttleworth CA, Kielty CM. Expression of latent TGF-beta binding proteins and association with TGF-beta 1 and fibrillin-1 following arterial injury. *Cardiovasc Res*. 2002;53:971–983. doi: 10.1016/s0008-6363(01)00512-0
43. Li L, Terry CM, Blumenthal DK, Kuji T, Masaki T, Kwan BC, Zhuplatov I, Leypoldt JK, Cheung AK. Cellular and morphological changes during neointimal hyperplasia development in a porcine arteriovenous graft model. *Nephrol Dial Transplant*. 2007;22:3139–3146. doi: 10.1093/ndt/gfm415
44. Misra A, Sheikh AQ, Kumar A, Luo J, Zhang J, Hinton RB, Smoot L, Kaplan P, Urban Z, Qyang Y, et al. Integrin β3 inhibition is a therapeutic strategy for supravalvular aortic stenosis. *J Exp Med*. 2016;213:451–463. doi: 10.1084/jem.20150688
45. Misra A, Feng Z, Chandran RR, Kabir I, Rotllan N, Aryal B, Sheikh AQ, Ding L, Qin L, Fernández-Hernando C, et al. Integrin beta3 regulates clonality and fate of smooth muscle-derived atherosclerotic plaque cells. *Nat Commun*. 2018;9:2073. doi: 10.1038/s41467-018-04447-7